SELF-HEALING POLYMERS

Introduction

Self-healing polymers are a new class of smart materials that have the capability to repair themselves when they are damaged without the need for detection or repair by manual intervention of any kind. Increasing demand for petroleum feed stocks used to produce polymer and the need for polymeric materials with improved performance in challenging applications continue to drive the need for materials with extended lifetimes. One way to extend the lifetime of a material is to mitigate the mechanism leading to failure. In brittle polymers, failure occurs through crack formation and propagation(1,2) and the ability to repair these cracks when they are still very small will prevent further propagation thus extending the lifetime of the material. Emerging self-healing technologies designed to give polymeric materials the capability to arrest crack propagation at an early stage thereby preventing catastrophic failures will go a long way in helping to increase the scope of applications of these materials.

Crack repair in polymeric materials by manual intervention has been well studied(3–9) and provides a good foundation for the discussion of self-healing polymers. Experiments performed using thermoplastics such as poly(methyl methacrylate) (PMMA) and polystyrene have shown that cracks can be healed by promoting the entanglement of polymer chains from each side of the crack face. The chain mobility required for this type of manually-induced healing is achieved either by heating the polymeric material above its T_g (3–9), or using solvents such as methanol and ethanol to promote depression of the effective T_g to below room temperature (10–14). However, as successful as these healing techniques were in laboratory studies, the scope of potential applications is limited to applications in which damage to a material can be easily observed and accessed for manual application of solvent or heating.

With the need for autonomic repair of materials without external intervention thus evident, more recent research has focused on developing fully self-healing systems. One approach to the design of such systems employs the compartmentalization of a reactive healing agent, which is then incorporated into a composite material. Thus, when a crack propagates through the material, it causes the release of the healing agent from the compartment in which it is stored into the crack plane where it solidifies and repairs the material.

The first basic application of this approach consisted of an epoxy matrix with suspended glass capillaries filled with either cyanoacrylate or a two-part epoxy resin (15). When a crack propagated through the cured epoxy matrix, the glass

capillaries were fractured and the cyanoacrylate monomer or the two-part epoxy, generally referred to as healing agents, were released into the crack plane where they reacted and polymerized. A significant recovery of the mechanical properties of the samples after they were allowed to heal suggests that the cracked material was effectively repaired by the polymerized healing agent. Since the healing requires only crack propagation as the trigger for the healing mechanism, it represents a truly autonomic or self-healing material. While a successful demonstration of self-healing, the labor-intensive process of manually filling capillaries and distributing them evenly throughout the matrix make this approach unsuitable for scale-up.

A key step toward a more practical approach to the design of self-healing materials was the use of microcapsules for compartmentalization of the healing agent. Microencapsulation is used widely for applications in carbonless copy paper, fragrance, food, and other industries. As such, microcapsules of various sizes employing various shell wall chemistries are already being produced on a very large scale. Microcapsules are well-suited to the application of crack healing because they can be engineered to be ruptured by a propagating crack and can repair those cracks at the micron scale before they propagate to produce more significant damage. Furthermore, because of their size, microcapsules can be easily added to and suspended in the matrix by stirring prior to use of the matrix in a specific application. Also, the size of the capsules, shell wall thickness, and chemistry can all be customized for various applications, thus rendering the use of microcapsules amenable to both existing and emerging materials and applications.

White and co-workers were the first group to report a microencapsulation-based self-healing system (16). Their work has inspired much progress in the area of self-healing materials research. For the purposes of the discussion presented herein, the recent literature on self-healing materials has been classified as autonomic healing and non-autonomic healing defined as follows:

(1) Autonomic healing: Fully self-contained and requiring no external intervention of any kind.
(2) Non-autonomic healing: Partially self-contained; healing capability is designed into the material, but additional external stimuli such as heat or uv-radiation is required for the healing to occur. This definition is intended to differentiate this level of autonomy in the healing mechanism from historical approaches such as solvent-welding, which required localization of the damage and manual application of solvent and/or heat.

The present work covers a variety of self-healing motifs, systems, and chemistries. The first example of a practical fully self-contained self-healing system based on microencapsulated dicyclopentadiene and Grubbs' catalyst particles embedded in an epoxy matrix,(16) formed the basis for further research on similar self-healing systems and thus forms the basis for the discussion presented herein. For all chemistries discussed, the efforts in compartmentalization of the reactants, evaluation of self-healing performance, and testing in relevant applications such as reinforced polymer composites and coatings are presented.

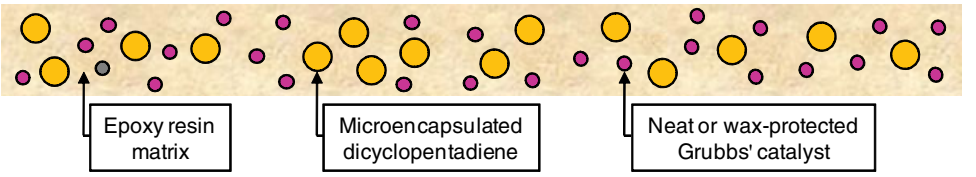

Fig. 1. Original microencapsulation-based self-healing system. Microencapsulated dicyclopentadiene is embedded in an epoxy resin containing Grubbs' catalyst which is capable of polymerizing the dicyclopentadiene. A propagating crack ruptures the microcapsules causing DCPD to be released into the crack plane where it comes in contact with and reacts with catalyst to form a polymer that bonds the crack faces and restores structural continuity.

Autonomic Healing

The recent literature on materials that can be classified as capable of autonomic healing can be further divided into sub-categories based on the self-healing concept employed. The subcategories include: One-capsule systems, dual-capsule systems, and microvascular or fiber network-based systems.

One-Capsule Systems. In 2001, White and co-workers reported the development of an epoxy-based material capable of autonomic repair after damage, without the need for any external intervention (16). Figure 1 illustrates the concept. Autonomic healing is accomplished by incorporating a microencapsulated healing agent (or monomer) and a chemical trigger (typically a catalyst or initiator) within an epoxy matrix. A propagating crack ruptures the microcapsules, releasing the healing agent into the crack plane by capillary action. Polymerization is initiated by contact with the embedded catalyst or initiator, bonding the crack faces, and restoring structural continuity.

Characteristics of the Ideal One-Capsule Self-Healing System. There are several requirements to consider in designing a truly self-healing system. These include long shelf-lives of the healing agent and the chemical trigger, low healing agent viscosity and volatility, rapid polymerization upon mixing of the healing agent and the chemical trigger at ambient conditions, low shrinkage upon polymerization, and good mechanical properties of the resulting polymer. Furthermore, since the stoichiometry of the healing chemistry cannot be controlled in the crack plane during a healing event, the initial rate of polymerization and overall degree of monomer conversion must be minimally dependent on the stoichiometric ratios of the reactants. This complex interplay of characteristics also includes the fact that for maximized healing properties to be observed, the monomer released into the crack plane must have sufficient time to cover the entire crack face, prior to the significant increase in viscosity due to the polymerization process, in order to have a continuous polymer layer that bonds the crack faces together. A comprehensive summary of the requirements for the design of microencapsulation-based self-healing systems is given in Table 1.

Self-healing Based on Ring Opening Metathesis Polymerization. Ring opening metathesis polymerization (ROMP) as initiated using first-generation Grubbs' catalyst, shown in Figure 2, appears to meet the most crucial requirements for the design of a self-healing system. The monomer is stable and can

Table 1. Characteristics Required for Designing Microencapsulation-Based Self-Healing Polymeric Materials(17,18)

Component	Required characteristics
Liquid healing agent	**Stability and shelf-life:** Must be stable enough to be encapsulated without reaction and must be stable within the microcapsule for long periods until it is released during a healing event **Deliverablity:** Must flow into the site of damage by capillary action, so it cannot be a highly viscous liquid. It must also remain in the site of damage long enough to react, so a highly volatile liquid is not desirable **Reactivity:** Once the healing agent comes in contact with the catalyst or second reactant, it must react quickly enough to provide healing in a reasonable time frame and to compete with nonproductive processes like evaporation, absorption into the matrix and side reactions **Shrinkage:** The resulting polymer should exhibit good adhesive characteristics to rebond the crack planes. Any volume shrinkage could result in the polymerized healing agent pulling away from the crack faces as it is being cured. **Physical and mechanical properties:** The incorporation of the healing agent in its encapsulated form should not introduce any deleterious effects to the matrix. Additionally the healing agent must demonstrate mechanical properties equal to or surpassing that of the matrix in its polymerized form **Thermal stability:** Must have a low freezing point and a high boiling point to minimize the likelihood of phase changes at various application or use-temperatures
Microcapsule shell wall	**Chemical compatibility:** Material must be chemically inert both to the core material within as well as the surrounding matrix chemistry **Mechanical properties:** To facilitate rupture during a healing event, the fracture toughness of the capsule shell wall material should be less than that of the matrix, but high enough to survive standard processing conditions **Dispersion:** Must facilitate or at the very least not create a hindrance to dispersion in the desired matrix **Thermal stability:** Must be thermally stable over a wide range of temperatures for a wider scope of applications

(*Continued*)

Table 1. (*Continued*)

Component	Required characteristics
Catalyst, curing agent, or reaction initiator	**Solubility:** The catalyst, curing agent or reaction initiator must dissolve rapidly in the liquid healing agent **Chemical compatibility:** Must be chemically stable to the matrix in which it is being incorporated to ensure activity when it is needed during a healing event **Reactivity:** Must promote rapid reaction with the healing agent. However, the reaction kinetics must not be faster than the dissolution kinetics as that would lead to self-limiting polymerization and inefficient use of the catalyst, curing agent or reaction initiator **Dispersion:** Must be well-dispersed throughout the matrix in order to ensure proximity to the microcapsules and efficient use of catalyst **Thermal stability:** The catalyst, curing agent or reaction initiator must be stable over a wide range of potential application or use-temperatures to ensure activity when it is needed during a healing event
Healing chemistry	**Stoichiometry:** Must be forgiving since it cannot be controlled in the crack plane during a healing event

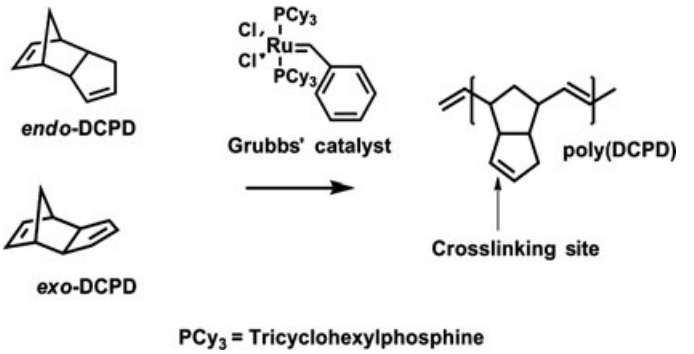

Fig. 2. ROMP of *endo*- and *exo*-DCPD with first generation Grubbs' catalyst.

be stored in a quiescent form in a microcapsule prior to reaction with the catalyst; the low viscosity of DCPD allows it to easily flow to the site of damage during a healing event; the conversion of monomer to polymer typically results in minimal shrinkage; and the resulting polymer, poly(dicyclopentadiene) (poly-DCPD) is a highly cross-linked polymer with impressive mechanical properties. The catalyst, bis(tricyclohexylphosphine) benzylideneruthenium (IV)di-chloride (first-generation Grubbs' catalyst) exhibits high metathesis activity with DCPD

monomer and acceptable chemical stability (19–21). Chemical stability of the catalyst is essential to ensure that the catalyst survives the processing conditions of sample preparation, remaining active to initiate ROMP during a healing event.

Microencapsulation of dicyclopentadiene. In ROMP-based self-healing systems, the DCPD monomer was encapsulated via an oil-in-water emulsion stabilized by poly(ethylene-co-maleic anhydride), using an acid-catalyzed reaction between urea and formaldehyde to form the poly(oxymethylene urea) shell wall (22,23). The resulting microcapsules are spherical and free flowing after drying. Microcapsule diameter is controlled over a wide range and is dependent on the rate of agitation of the emulsion. As the rate of agitation increases, a finer emulsion is achieved and the average diameter of the resulting microcapsules decreases. Agitation via mechanical stirring facilitates the production of capsules ranging from 1000 to 10 μm (22). However, the recent use of ultrasonification and miniemulsion techniques have led to the production of capsules as small as 200 nm (24).

Incorporation of Catalyst. While the liquid healing agent was first encapsulated prior to being embedded into the matrix, the first-generation Grubbs' catalyst was embedded directly into the matrix in its neat solid form. In initial reports on ROMP-based self-healing systems (16,23), the stability of the catalyst to the EPON® 828 epoxy resin and the diethylenetriamine (DETA) curing agent was investigated using proton nuclear magnetic resonance (^{1}H NMR) to ensure that the catalyst would remain active until it was needed in a later healing event. The catalyst was found to retain its activity in the presence of the resin alone, but was rapidly deactivated in the presence of the curing agent alone. It was later suggested that this deactivation could be due to the displacement of the phosphine ligands in the first-generation Grubbs' catalyst by the DETA to form a short-lived bis-amine ruthenium complex that quickly decomposed (25,26). However, the catalyst retained some activity in the presence of the EPON® 828/DETA mixture during cure as increasing viscosity and the competitive reaction between the epoxide and the amine worked together to decrease the concentration of free amine available to react with and decompose the catalyst. Two factors that affect the stability of the catalyst in the EPON® 828/DETA mixture during cure are the size and morphology of the catalyst particles. In the case of the size of the catalyst particles, it was found that smaller particles ($<$75 μm) dissolved too easily in the curing epoxy system due to their increased surface area and were thus deactivated by free amine present in the curing reaction mixture. On the other hand, while significantly more stable in the curing epoxy system, larger particles presented the possibility of encumbered dissolution in the DCPD monomer during a healing event (27). Morphology was also found to play a role in catalyst stability as higher surface area morphologies produced via freeze-drying techniques were more prone to deactivation than more robust lower surface area morphologies obtained from the manufacturers Strem Chemicals and Sigma-Aldrich (25,27).

Mechanical Characterization:Quasi-Static Fracture Conditions. In the design of self-healing polymeric materials, it is essential to demonstrate the functional recovery of the initial (typically referred to as virgin) mechanical properties in some fashion. Significant effort has been made to develop a set of experimental protocols that can be used to evaluate self-healing materials in both quasi-static and dynamic fracture conditions.

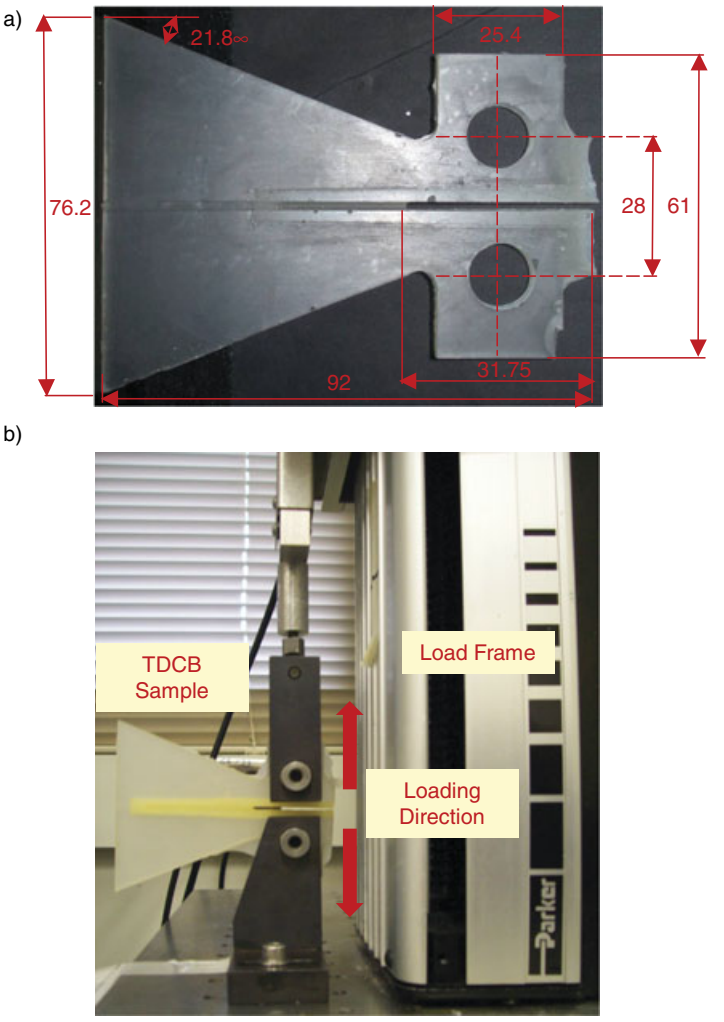

Fig. 3. (**a**) Image and basic dimensions of a TDCB specimen in mm; (**b**) TDCB specimen mounted in a load frame prior to fracture testing.

For quasi-static fracture conditions, the healing efficiency is defined as a function of the recovery of fracture toughness (16,23). The fracture toughness (K_{Ic}) for both the virgin and healed samples is determined using a tapered double-cantilever beam (TDCB) geometry (Fig. 3**a**), which provides a crack-length-independent measure of the fracture toughness and allows the fracture toughness to be related to the peak load at failure (P_c) by a simple geometric coefficient. Therefore, the healing efficiency for quasi-static conditions (η) can be related to both the fracture toughness and the peak fracture load using equation (1):

$$\eta = \frac{K_{Ic_{\text{healed}}}}{K_{Ic_{\text{virgin}}}} = \frac{Pc_{\text{healed}}}{Pc_{\text{virgin}}} \tag{1}$$

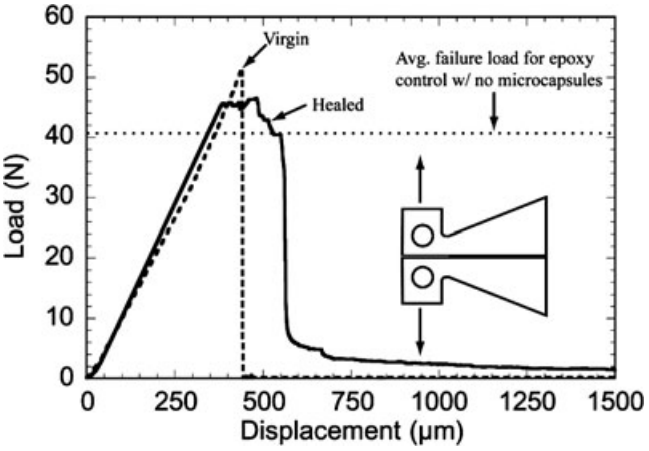

Fig. 4. Load-displacement data for a virgin and healed TDCB self-healing epoxy sample containing 2.5 wt% first generation Grubbs' catalyst and 5 wt% DCPD capsules. The healing efficiency is approximately 90% after 48 hours at room temperature. Inset: Schematic of TDCB sample. Reprinted from E.N. Brown, N.R. Sottos, and S.R. White, *Exp. Mech*. **42**, 372–379 (2002) with permission from Springer.

Evaluation of self-healing performance thus typically begins with a virgin fracture test of a previously untested or undamaged TDCB sample. A precrack is then introduced to sharpen the crack tip of the sample. The sample is then mounted on a load frame and loaded under displacement control causing the precrack to propagate along the centerline of the sample until failure (Fig. 3**b**). The crack is then closed and allowed to heal at room temperature for a specified period of time. After healing, the sample is loaded again to failure. The resulting fracture data (peak fracture load and/or fracture toughness) are compared using equation (1) to determine a value for the healing efficiency. Figure 4 exhibits a representative load-displacement data for a virgin and healed self-healing epoxy sample. Using this protocol, conclusive demonstration of self-healing capability for an epoxy sample containing microcapsules filled with DCPD and solid Grubbs' catalyst particles was achieved (16,23). Using optimized concentrations of microcapsules and catalyst, healing efficiencies as high as 90% have been reported (23).

Mechanical Characterization: Dynamic Fracture Conditions. In dynamic fracture conditions, which are more typical in practice, the healing efficiency calculated for quasi-static conditions no longer applies. Instead, the healing efficiency is defined in terms of the life extension factor (λ) as shown in equation (2), (28)

$$\lambda = \frac{N_{\text{healed}} - N_{\text{control}}}{N_{\text{control}}} \tag{2}$$

where N_{healed} is the total number of fatigue cycles to failure for the self-healing sample and N_{control} is the total number of fatigue cycles to failure for a similar sample without self-healing functionality. The fatigue of microcapsule-based self-healing epoxies utilizing ROMP chemistry has been studied in a number of

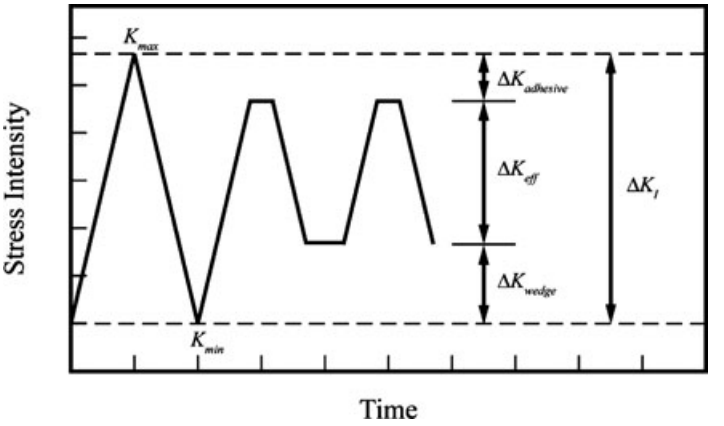

Fig. 5. Schematic of cyclic-loading profile showing the stress intensity-reducing effects of crack-tip shielding mechanisms activated by the self-healing process. Reprinted from E.N. Brown, S.R. White, and N.R. Sottos, *Compos. Sci. Tech*. **65**, 2466–2473 (2005) with permission from Elsevier.

recent articles (28–30). These studies all demonstrated a significant extension of fatigue life when self-healing chemistry was incorporated into an epoxy resin in comparison to the neat resin material.

As was the case with the quasi-static performance tests, fatigue life extension due to self-healing was evaluated using the TDCB specimen geometry. After precracking the samples, load was applied using a triangular waveform varying between maximum crack-tip stress intensity, $K_{\max}$ and minimum stress intensity, $K_{\min}$ as shown in Figure 5. The use of the crack-length independent TDCB geometry ensured a constant growth rate over the majority of the specimen, in the absence of any other mechanisms contributing to shielding of the crack growth.

Several mechanisms work in concert to improve the fatigue life of a self-healing material by reducing the crack-tip stress intensity. In a virgin undamaged sample, a crack tip is subjected to the global stress intensity, ΔK_I (Fig. 5), as dictated by the far-field loading conditions. When self-healing begins to occur in the crack plane, a wedge of polymerized healing agent forms at the crack tip. The resulting effective stress intensity driving the crack tip forward (ΔK_{eff}) is significantly reduced relative to the global stress intensity (ΔK_I) since the wedge prevents full loading ($\Delta K_{adhesive}$) and unloading (ΔK_{wedge}) of the crack tip. These mechanisms are most active when the healing agent released into the crack plane has sufficiently polymerized. However, the presence of a liquid healing agent in the crack plane also introduces hydrodynamic crack-tip shielding but is less effective at retarding crack growth (28).

Fatigue of the ROMP-based self-healing system highlights the important role of the interplay between chemical and mechanical kinetics that are likely to characterize any self-healing system. The ability to retard and ultimately arrest fatigue cracks hinges on the ability of the healing chemistry to produce polymer in the crack plane at a rate that is comparable to the rate of crack propagation (30). In a sample that is exposed to high frequency or high stress level fatigue cycles, the healing kinetics are not fast enough to significantly retard crack

growth. However, if rest periods are incorporated into the loading cycle, then sufficient time for healing is maintained and significant life extension can be achieved. Modification of the kinetics of the healing chemistry and hence the polymerization rate of monomer released into the crack plane can have an impact on the healing performance as shown in Figure 6**a**. For this fatigue cycle regime, faster healing kinetics results in greater life extension. As can be expected, if a sample is fatigued at low enough frequency and/or stress levels, the healing chemistry kinetics dominate and the crack is effectively arrested (Fig. 6**b**).

Microcapsule Induced Toughening. Brown and co-workers have demonstrated that the incorporation of microcapsules into an epoxy matrix do not adversely affect the mechanical properties of the matrix. On the contrary, the fracture toughness measurements of samples cast from an EPON 828 epoxy resin system were observed to increase with concentration up to an optimal concentration that is dependent on the average diameter of the microcapsules. Overall, the incorporation of microcapsules containing DCPD into epoxy samples yielded up to a 127% increase in fracture toughness, outperforming samples containing similar concentrations of silica microspheres, or solid urea-formaldehyde particles (31).

Application in Reinforced Polymer Composites. A logical application for self-healing technology is in fiber-reinforced composites made from brittle polymers, which are susceptible to microcracking when subjected to thermomechanical loading common to their application environment. Transverse cracks and delaminations can also occur in laminated composites even at modest levels of impact. Regardless of the damage mechanism, severely damaged structural components are typically replaced entirely, while less extensive damage is repaired. Common repair methods typically require costly and time-consuming manual intervention by a trained technician. Incorporation of self-healing technology capable of healing microcracks and delaminations in reinforced composites will lead to life extension of those composites and the applications in which they are used. Such life extension will lead to significant decrease in maintenance cost and loss of productivity associated with the sidelining of expensive assets for maintenance.

The presence of fiber reinforcement in a brittle polymer matrix increases the number of potential damage modes and the complexity of the healing process. Microcracks in the resin portion of a reinforced composite can be healed in a fashion similar to the non-reinforced resin matrix previously described. However, the development of a self-healing system that addresses the other damage mechanisms of a composite is a fundamentally more challenging proposition (32). To address the quasi-static mechanical characterization of a self-healing composite, a width-tapered double cantilever beam (WTDCB) testing protocol aimed at the evaluation of delamination damage was developed. The WTDCB geometry (Fig. 7) provides a crack length independent measure of fracture toughness and the healing efficiency (η) is the ratio of the peak fracture load of the healed sample to the peak fracture load of the virgin sample.

Repair of relatively large-scale delaminations in a self-healing fiber-reinforced structural polymer composite was achieved by incorporating urea-formaldehyde microcapsules containing DCPD and first-generation Grubbs' catalyst particles in a carbon-fiber-reinforced epoxy matrix (33). With no manual

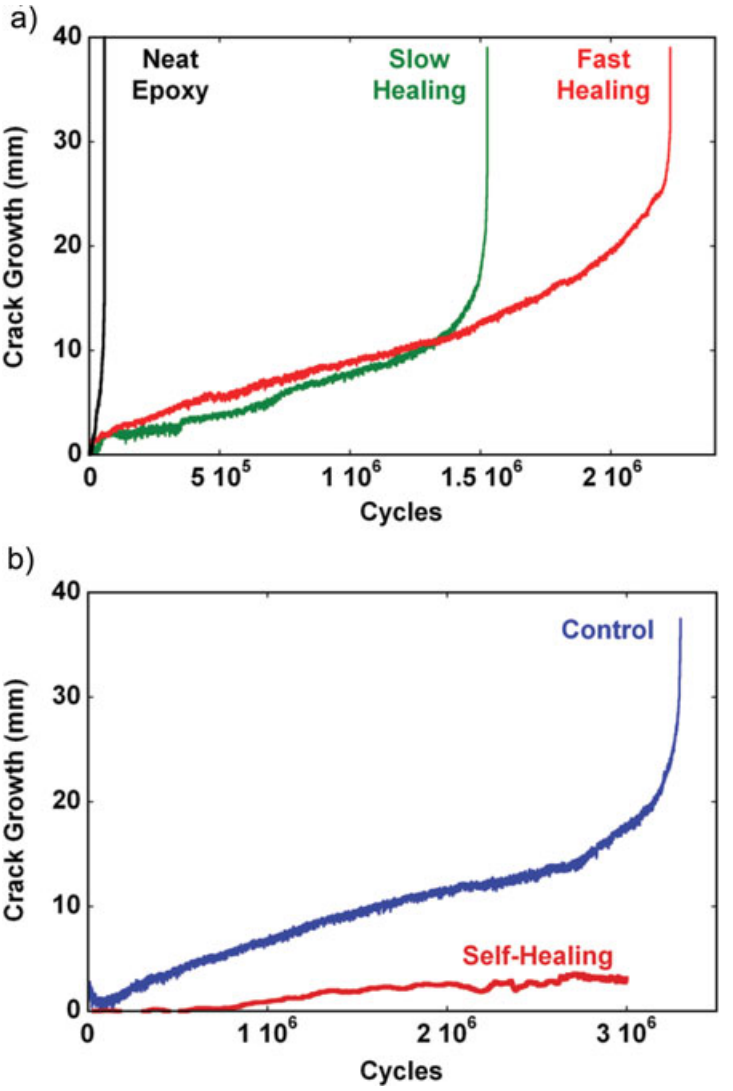

Fig. 6. Fatigue testing data for TDCB self-healing epoxy samples containing 20 wt% microcapsules containing DCPD and 5 wt% wax microspheres containing 5 wt% Grubbs' catalyst. Control samples contain 20 wt% microcapsules and no catalyst. (**a**) Comparison of fatigue life extension observed for varying healing kinetics (fast and slow, where faster chemical kinetics is due to the utilization of a rapidly dissolving catalyst polymorph). Life extension for the slow healing was approximately 1300% while that of the fast healing was approximately 2000%; (**b**) healing kinetics dominates at low stress levels and complete crack arrest is achieved (ie, the life extension is infinite). Reprinted from A.S. Jones, J.D. Rule, J.S. Moore, N.R. Sottos, and S.R. White, *J. R. Soc. Interface* **4**, 395–403 (2007) with permission from The Royal Society.

intervention, a recovery of close to 50% was achieved after healing for 48 hours at room temperature, and upon elevating the healing temperature to 80°C for 48 hours, the healing efficiency dramatically increased to over 75%. To the best of our knowledge, no data on the self-healing performance of a ROMP-based

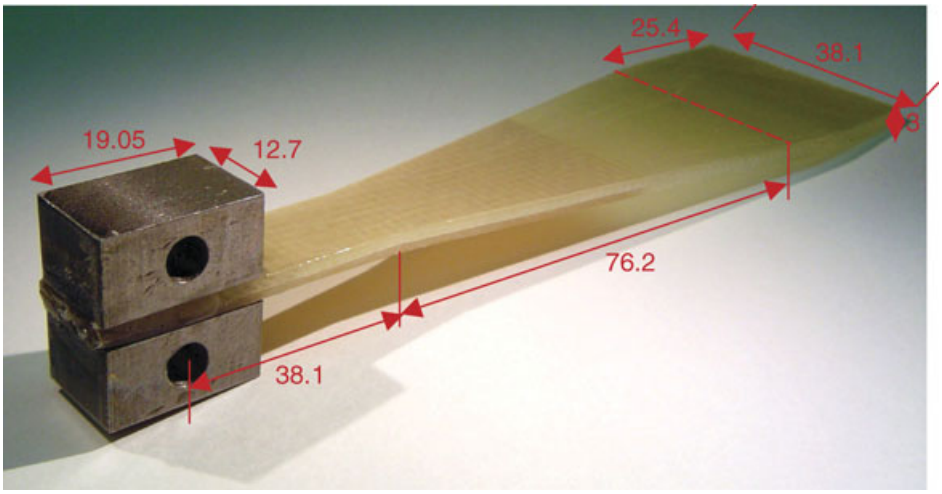

Fig. 7. Image of WTDCB sample with the dimensions given in mm. A Teflon® insert is included to initiate a delamination along the specimen midplane. A nontapered region (25.4 mm) at the end of the specimen is included for crack arrest.

reinforced polymer composite in fatigue loading conditions has been reported to date. However, it is very likely that as was the case with the results of the quasi-static healing tests, the self-healing performance of this system will be closely aligned with the self-healing performance of the unreinforced resin.

Another set of damage mechanisms that composites can be exposed to are those created by out-of-plane impact events, which can significantly compromise the integrity of the structure. This type of damage is often hidden or barely visible, making it difficult to detect. Damage from impact can also include significant fiber breakage, matrix cracking, and gross delaminations. While self-healing technology is unlikely to address all these damage mechanisms, specific damage modes can be targeted by a careful choice of the appropriate size scale of the self-healing components. In a recent study by Patel and co-workers (34), glass fiber-reinforced epoxy composites containing DCPD-filled urea-formaldehyde microcapsules and first-generation Grubbs' catalyst were investigated for mitigation of impact damage. A dual microcapsule size scale approach (microcapsules of 35 μm, and 180 μm diameter) was used to provide both an increased uniformity of dispersion and sufficient healing agent delivery. Using a drop weight impact tester, for low-velocity impact testing, delaminations caused by low-velocity impact testing were reduced by 51% as quantified by cross-sectional crack length reduction.

Improvements to ROMP-Based Self-Healing Systems. Much research has been performed on ROMP-based self-healing systems since they were first reported in 2001. The improvements discussed herein were the result of studies spanning a broad range of parameters including but not limited catalyst protection and alternative catalysts and monomers.

Catalyst Protection. One of the limitations to the practical utility of the original design of ROMP-based self-healing systems was the need to use a

relatively high concentration (2.5 wt%) of catalyst for good self-healing performance to be observed. The high concentration used was made necessary by the fact that some of the catalyst is deactivated by DETA during the processing of the material, as well as the need to increase the degree of dispersion of the catalyst and thus increase the likelihood that enough catalyst will be present in a specific area of damage when necessary. By embedding the first-generation Grubbs catalyst in wax to form wax microspheres, Rule and co-workers(35) achieved effective self-healing at dramatically lower catalyst concentrations (0.25 wt%). The wax microspheres containing first-generation Grubbs' catalyst were formed using a hydrophobic congealable disperse phase encapsulation procedure (35). In this procedure, a mixture of molten wax and the catalyst is poured into a hot, rapidly stirring, aqueous solution of poly(ethylene-co-maleic anhydride) or poly(vinyl alcohol). After stirring for a few minutes, rapid cooling of the suspension of catalyst and molten wax yields wax microspheres containing particles of first-generation Grubbs' catalyst. Results obtained from a quasi-static evaluation of the healing performance of TDCB samples containing catalyst microspheres instead of neat catalyst particles suggests that the use of catalyst microspheres improves the healing efficiency by serving two purposes. Firstly, by improving the dispersion of the catalyst in the epoxy matrix, the presence of regions of incomplete healing due to nonuniform catalyst availability is minimized. Secondly, the wax protects the catalyst from deactivation upon exposure to DETA during curing of the resin, effectively increasing the amount of active catalyst available for the initiation of polymerization during a healing event.

Alternative Catalysts and Monomers. As shown in Figure 2, DCPD can exist as the *endo* or *exo* isomer. While the original work on ROMP-based self-healing systems described thus far used the commercially available *endo*-isomer (commercially available DCPD > 95% *endo*), the *exo*-isomer is known to exhibit much faster olefin metathesis reaction rates with first-generation Grubbs' catalyst (36). For most applications of self-healing technology envisioned, it would be preferable to have the fastest healing kinetics possible so long as the healing efficiency is not compromised. However, as already discussed, the design of self-healing systems is a complex problem that involves physical parameters such as monomer transport, mixing, catalyst dissolution, and catalyst transport in addition to the healing chemistry. The use of the much more reactive *exo*-DCPD led to rapid gelation and insufficient time to completely dissolve the catalyst, a self-limiting type of polymerization, a low degree of cure and thus a low healing efficiency due to the inefficient employment of the catalyst (37). Jones and co-workers showed that complete dissolution of first-generation Grubbs' catalyst occurs in the range of 5–10 minutes (27). This dissolution rate is acceptable for self-healing with *endo*-DCPD, which gels in about 20 minutes at room temperature. For *exo*-DCPD which gels in seconds, much of the catalyst remains undissolved and the DCPD simply gels around the catalyst particles, leading to a nonuniform layer of polymer in the crack plane and thus low healing efficiency (37,38).

Mauldin and co-workers were able to demonstrate however, that the desired combination of faster healing kinetics and high healing efficiency could be achieved by blending the *exo*- and *endo*-isomers of DCPD at appropriate levels (36). Healing efficiencies as high as 60% were observed in systems that contained first-generation Grubbs' catalyst embedded in wax microspheres

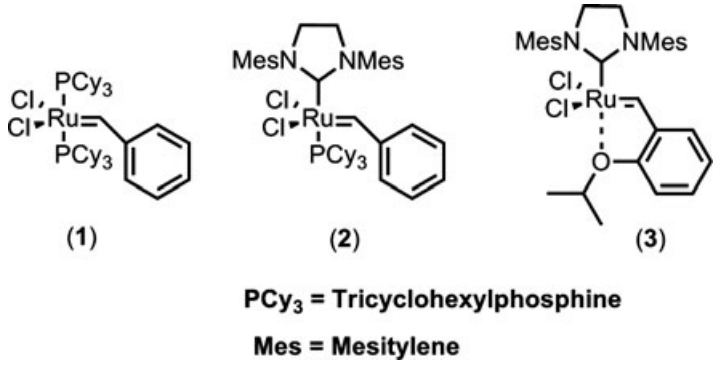

Fig. 8. Ruthenium catalysts compared.

incorporated at an overall catalyst concentration of 0.25 wt%, and microcapsules containing a blend of *endo*- and *exo*-DCPD incorporated at a concentration of 10 wt%. A ratio of 60:40 *exo/endo* was found to be optimal for high healing efficiencies and faster healing kinetics. In addition to the accelerated polymerization, *exo*-DCPD exhibits different phase transition properties in comparison to *endo*-DCPD. The *exo*-DCPD monomer has a freezing point of less than -50°C (compared to 15°C for *endo*-DCPD), making it a potential healing agent for cryogenic applications. Initial fracture tests for samples containing *exo*-DCPD as the monomer performed in a cold room environment (0–4°C) showed no degradation in healing capability as compared to the same tests performed at ambient conditions where the reaction occurred too rapidly (36). A blend of *exo*- and *endo*-DCPD has also been used with wax-protected Grubbs' catalyst in the development of a self-healing system for the epoxy vinyl ester resin Derakane 510A-40. The wax in this case served to protect the catalyst from free-radicals generated *in situ* during the curing of the resin (39).

With the successful demonstration of ROMP-based self-healing systems initiated by first-generation Grubbs' catalyst, Wilson and co-workers compared this catalyst to two additional ruthenium metathesis catalysts (second generation Grubbs' catalyst and Hoveyda-Grubbs' second generation catalyst) (25). All three catalysts compared are shown in Figure 8. The catalysts were compared across a range of properties including ROMP initiation kinetics, chemical stability to epoxy curing agents, thermal stability, and ROMP reactivity with alternative healing agents.

With regards to the initiation of ROMP kinetics using DCPD as the monomer, the Hoveyda-Grubbs' second-generation catalyst proved to be significantly more reactive with over 60% of DCPD conversion observed within the first 5 minutes. The second-generation Grubbs' catalyst exhibited the slowest reaction kinetics in bulk polymerization, an observation which is in contrast with the performance observed for similar reactions performed in solution (25,40).

Both second-generation Grubbs' and Hoveyda-Grubbs second-generation catalysts exhibited significantly improved stability to exposure to DETA during the epoxy curing process relative to the first-generation catalyst especially when incorporated into the epoxy in the freeze-dried form. Identical disparate samples

containing freeze-dried catalysts at 2.5 wt% and DCPD capsules at 10 wt% were fractured and healed for 24 hours. When retested for evaluation of the healing efficiency, the first-generation Grubbs' catalyst exhibited no healing, while both the second-generation and the Hoveyda-Grubbs second-generation catalysts exhibited some recovery (approximately 28 N and 20 N) of virgin mechanical properties. This observation is consistent with a recently published study that suggests that the presence of the N-heterocyclic carbene ligand in the second-generation derivatives of Grubbs' catalysts, as opposed to the tricyclohexyl phosphine ligands found in the first-generation derivatives, yields complexes that are more stable to primary amines (26).

The evaluation of these three catalysts also yielded the observation that alternative ROMP monomers could be used to improve self-healing performance by using a second monomer with the potential for improved non-covalent interaction with the matrix. Wilson and co-workers found that by carefully matching the surface properties of a particular matrix to the selection of the healing agent or blend of monomers used, improved self-healing performances could be observed. Matrices with lower contact angles for example exhibited higher healing efficiencies with a more polar ROMP co-monomer such as norbornene carboxylic acid, while those with higher contact angles exhibited higher healing efficiencies with a nonpolar ROMP co-monomer such as ethylidene norbornene (Fig. 9) (26).

Another alternative ROMP catalyst that has been evaluated for use in self-healing materials systems is tungsten hexachloride (WCl_6). When used with phenylacetylene as a co-activator and nonylphenol as a dissolution agent, the WCl_6 system offers a cost-effective alternative to Grubbs' catalyst that is widely available and has a melting point of 275°C, which is significantly higher than 153°C previously reported for first generation Grubbs' catalyst (41). The best self-healing performance of this system reported to date was for epoxy samples containing 12 wt% WCl_6 particles and 15 wt% *endo*-DCPD microcapsules, which recorded a maximum healing efficiency of approximately 20% (41). However,

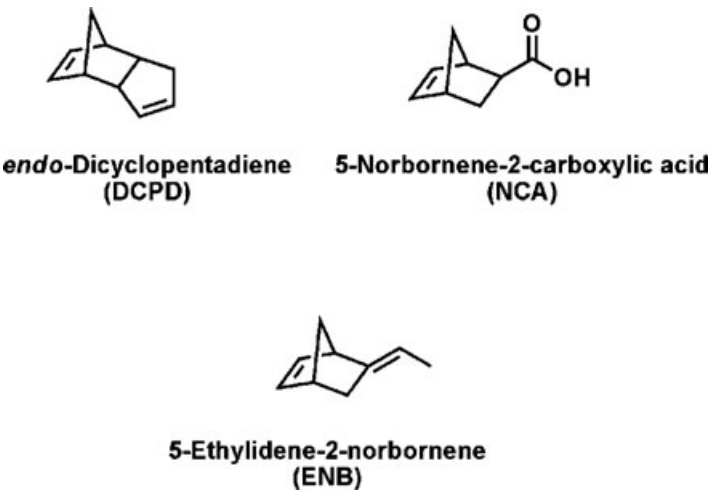

Fig. 9. Combination of healing agents used to evaluate noncovalent adhesion promotion.

further research is made necessary by the potential commercial viability of a system incorporating WCl_6; which has been demonstrated in the Metton (Metton America) liquid molding two-part resin system based on the polymerization of *endo*-DCPD with WCl_6 and a co-activator for reaction injection molding of high volume parts.

Effect of Microcapsule Size. With a view toward applications that make smaller microcapsules necessary, Rule and co-workers evaluated the effect of microcapsule size on self-healing performance (42). To relate the amount of healing agent delivered into the crack plane to the diameter of the microcapsules, Equation (3)was derived:

$$\bar{m} = \rho_s \Phi d_c \tag{3}$$

where $\bar{m}$ is the amount of healing agent delivered normalized by the area of the crack face, ρ_s is the density of the sample, Φ is the mass fraction of microcapsules and d_c is the diameter of the microcapsules. Rule and co-workers confirmed this relationship through a series of fracture tests in which various amounts of healing agent were injected into the crack plane of samples already containing wax-protected Grubbs' catalyst particles, and microcapsules of sizes ranging from 14 to 386 μm were used. An understanding of this relationship led to better optimization of capsule size and concentrations for various damage sizes.

Solvent-Induced Self Healing. Although the viability of WCl_6-catalyzed ROMP chemistry was successfully demonstrated on a commercial scale in the Metton liquid molding two-part resin system described above; the healing efficiencies observed, when this chemistry was used in the design of a self-healing epoxy material, were low presumably due to the sensitivity of the WCl_6 to moisture. Protection in wax preserved some catalyst activity, but also led to plasticization of the epoxy matrix thus compromising its mechanical integrity. These limitations led to the development of solvent-induced self-healing systems as simple, cost-effective solutions to self-healing in epoxies.

Solvent-induced self-healing systems are one-capsule systems in which microcapsules containing solvent are embedded in the epoxy prior to molding or use in the intended application (Fig. 10). When a crack propagates through an epoxy material formulated as such, it ruptures the microcapsules causing the solvent to be released into the crack plane. Once in the crack plane, the solvent penetrates the epoxy network to elute out unreacted amines and amine end-groups as well as unreacted epoxy resin which react further to heal the crack. Preliminary reference tests in which epoxy TDCB samples were fractured and healed

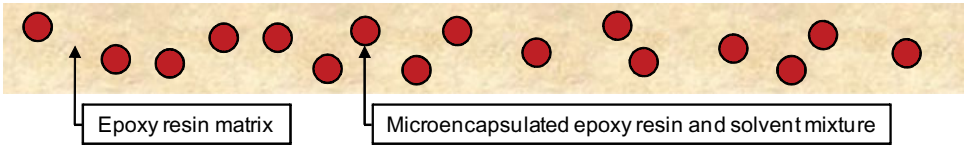

Fig. 10. Solvent induced healing system. A propagating crack ruptures the microcapsules releasing a blend of epoxy resin and solvent into the crack plane where the epoxy penetrates the matrix network to elute out and react with residual unreacted amine groups.

by manual injection of solvent, demonstrated a relationship between polarity of the solvent and its ability to heal the epoxy matrix (42). Although the nature of this relationship remains unclear, the five solvents that exhibited the highest healing efficiencies were nitrobenzene, *N*-methyl pyrrolidone (NMP), dimethylacetamide (DMA), dimethylformamide (DMF) and dimethyl sulfoxide (DMSO). No indication of healing ability was observed on both extremes of the polarity spectrum with cyclohexane, hexanes, formamide, and water demonstrating no ability to promote recovery of mechanical properties.

Due to their polarity, the five best-performing solvents noted above could not be encapsulated using the standard urea-formaldehyde encapsulation procedure already discussed. After several unsuccessful attempts at reverse-phase encapsulation procedures to encapsulate these solvents, chlorobenzene (the next best-performing solvent that could be encapsulated) was encapsulated using the standard urea-formaldehyde procedure. Samples containing chlorobenzene microcapsules exhibited up to 82% healing efficiency, while control samples containing nonpolar solvents such as xylenes and hexanes exhibited healing efficiencies of 38% and 0%, respectively (43).

An important improvement to the first attempt at solvent-induced self-healing systems was the realization that the microencapsulation of a mixture of an epoxy resin and a solvent could yield more efficient self-healing systems (44). In addition, nontoxic solvents such as phenyl acetate and ethyl phenyl acetate were used instead of the significantly more toxic chlorobenzene. Overall, for epoxy samples containing 15 wt% microcapsules, the combination of the epoxy resin, and solvent in the capsules when compared to just solvent alone led to an increase of about 20% in healing efficiency (44). Characterization of the fracture planes of healed samples formulated with microcapsules containing solvent and brominated epoxy by energy dispersive x-ray spectroscopy (EDS) confirmed the release of the epoxy from the ruptured microcapsules and onto the fracture plane during a healing event. It is interesting to note that the samples prepared for these experiments exhibited the capability for multiple repair events at the same damage location. After the first healing event, the samples were retested after 7 days or longer and high healing efficiencies were observed for the second healing event. Repeated testing of these samples over time showed a decrease in the healing efficiency with each successive healing event. A maximum of 3–5 healing events were observed over a series of experiments. The reduction in healing efficiencies was attributed to local depletion of healing agent as well as a decrease in the amount of residual amines available for reaction with the epoxy (44).

Dual-Capsule Systems. Dual-capsule systems became a necessity in an attempt to compartmentalize separate chemistries comprised of liquid reactants for use as self-healing chemistries. These systems are characterized by the additional complexity presented by the need for two distinct liquids to mix to an appreciable extent in the site of damage during a healing event. Two polydimethylsiloxane (PDMS)-based chemistries have been used to develop dual-capsule systems including hydroxyl-terminated PDMS condensation and hydrosilylation.

Polydimethylsiloxane Condensation. The development of PDMS-based self-healing chemistries was a significant step toward the realization of more chemically stable chemistries. The first attempt at compartmentalization of this chemistry for self-healing purposes was based on tin-catalyzed

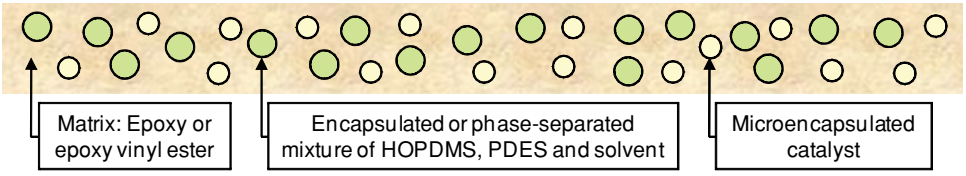

Fig. 11. Silanol condensation-based self-healing system. The mixture of HOPDMS, PDES, and solvent is either encapsulated or phase-separated. The catalyst is encapsulated in polyurethane microcapsules. Damage through the matrix ruptures the microcapsules and their contents mix in the crack plane initiating a polymerization that seals the crack.

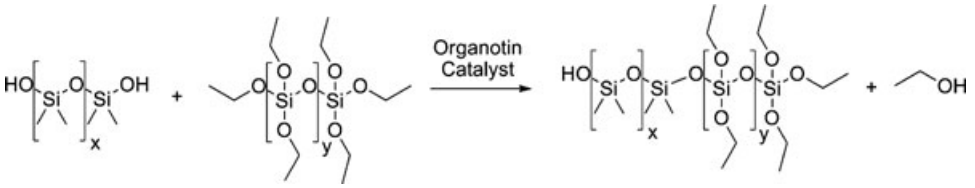

Fig. 12. Silanol polycondensation. A hydroxyl-terminated PDMS polymer chain reacts with an ethyl silicate (PDES) in the presence of an organotin catalyst. The reaction results in a crosslinked network and releases ethanol as a condensation product.

polycondensation of phase-separated droplets containing hydroxyl end-functionalized poly(dimethylsiloxane) (HOPDMS) and poly(diethoxysiloxane) (PDES) (45). The catalyst, di-n-butyltin dilaurate (DBTL) was encapsulated in polyurethane microcapsules and embedded in an epoxy vinyl ester matrix. Figure 11 shows a schematic diagram illustrating this approach. As was the case with previous systems, a crack propagating through the matrix would rupture the microcapsules containing the catalyst causing their contents to be released into the crack plane where they would react with the phase-separated HOPDMS and PDES. The reaction is a polycondensation reaction in which the PDES serves as the cross-linking agent (Fig. 12). This system possesses a number of important advantages over ROMP-based systems including stability in humid and wet environments, higher thermal stability (facilitating healing in higher-temperature thermoset applications) and the components are widely available and much more economical.

Incorporation of HOPDMS and PDES into the Matrix. After confirming immiscibility of the HOPDMS/PDES healing agent system with the epoxy vinyl ester by elemental analysis, the epoxy vinyl ester resin was vigorously mixed with the HOPDMS, PDES, and an adhesion promoter. The size distribution of the phase-separated HOPDMS/PDES mixture after mechanical stirring at 600 RPM ranged from 1–20 μm. The droplet size was not as dependent on stirring rate as was the case in microencapsulation and did not vary significantly in samples stirred between 100 and 2000 RPM (45). The adhesion promoter was included to promote adhesion of the PDMS polymer formed in the crack plane after a healing event and the epoxy vinyl ester matrix.

Microencapsulation of the Catalyst. The microcapsules containing the catalyst were formed through interfacial polymerization and were comprised of

a polyurethane shell wall and a core mixture of DBTL and chlorobenzene. The urethane prepolymer was synthesized through the reaction of toluene 2,4-diisocyanate and 1,4-butanediol in cyclohexanone at 80°C for 24 hours (46). The cyclohexanone was then evaporated off under vacuum at 100°C. The resulting urethane prepolymer was then dissolved in the mixture of DBTL and chlorobenzene and added to a mixture of water and 15 wt% gum Arabic. The resulting mixture was stirred for 30 minutes at 70°C and 30 wt% (relative to the amount of prepolymer) of ethylene glycol (chain extender) was added. Spherical microcapsules, containing DBTL dissolved in chlorobenzene, were obtained after an additional 2 hours at 70°C and stirring at 1000 rpm. The sizes of microcapsules produced using this procedure are strongly dependent on stirring rate and ranged from 50 μm to 450 μm for stirring rates ranging from 2000 to 500 RPM, respectively.

Evaluation of Self-Healing Performance. To obtain the self-healing epoxy vinyl ester, the HOPDMS, PDES, and adhesion promoter were added to the epoxy vinyl ester resin (Derakane 510A-40) along with benzoyl peroxide (BPO) which served as the free radical polymerization initiator. After thoroughly stirring to ensure complete dissolution of the BPO, the DBTL capsules were then mixed in followed by addition of dimethyl aniline (DMA), which served as the promoter for the curing of the vinyl ester matrix. The resulting resin mixture was then carefully poured into TDCB specimen molds. The cured specimen were fractured and healed as already described. Healing efficiencies were determined using Equation (1). The maximum healing efficiency observed for this system was achieved in samples containing 12 wt% HOPDMS/PDES, 4 wt% adhesion promoter, and 3.6 wt% microcapsules. Relative to the neat epoxy vinyl ester, the recovery of virgin fracture toughness was about 46%.

Application to Self-Healing Coatings. A version of the system described above was evaluated for performance as a self-healing coating system (46). The initial system evaluated was comprised of the epoxy vinyl ester used above with BPO and DMA as the initiator and promoter respectively, 12 wt% of phase-separated HOPDMS/PDES healing agent, 3 wt% polyurethane-encapsulated dimethyldineodecanoate tin (DMDNT) catalyst solution, and 3 wt% methylacryloxy propyltriethoxy silane adhesion promoter. The HOPDMS/PDES healing agent blend was a mixture of 96 vol% HOPDMS and 4 vol% PDES, and the catalyst solution containing 5 wt% DMDNT in chlorobenzene. After thorough mixing, this coating system was applied on cold-rolled steel samples. These samples, as well as control samples prepared similarly (but excluding the phase-separated healing agent and the catalyst microcapsules) were scribed by hand using a razor blade and allowed to heal at 50°C for 24 hours. The samples were then immersed in a 5 wt% sodium chloride solution for a specified period of time. All the control samples were observed to rapidly corrode within 24 hours, and exhibited extensive rust formation in and around the scribed region of the sample (Fig. 13**a**). In dramatic contrast, the self-healing samples showed no visual evidence of corrosion even after 120 hours after exposure (Fig. 13**b**). Additional control experiments revealed the importance of the incorporation of both the healing agent and the catalyst as removal of either of the two additives required for self-healing resulted in samples that exhibited rust (Figs. 13**c** and 13**d**).

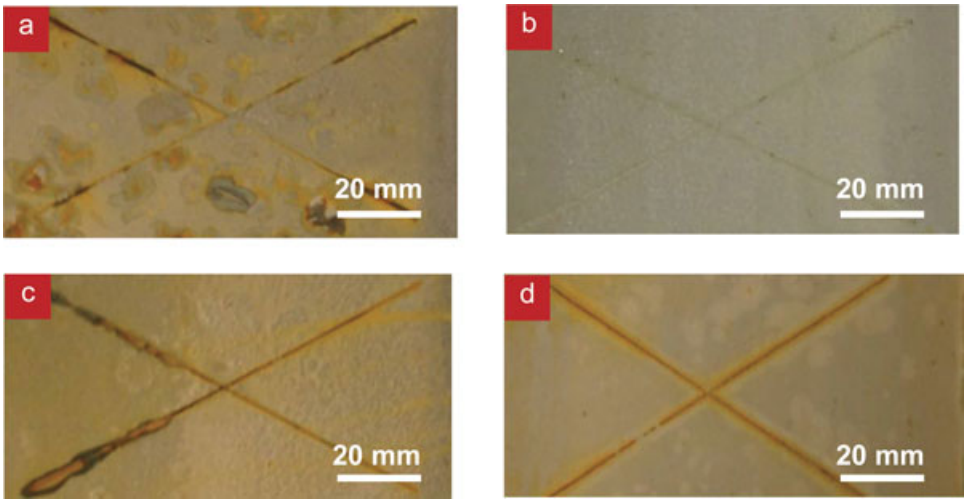

Fig. 13. Vinyl ester resin coating containing (**a**) only adhesion promoter (control sample); (**b**) the complete self-healing system including HOPDMS, PDES, catalyst microcapsules and adhesion promoter; (**c**) HOPDMS, PDES, and adhesion promoter; (**d**) catalyst microcapsules and adhesion promoter. All samples were healed at 50°C.

While the model to self-healing coatings described exhibited impressive results, some limitations were apparent. First, the phase-separated PDMS healing agents are in direct contact with the matrix curing chemistry and are thus susceptible to potentially adverse reactions. For example, the amine curing agents used in many epoxies catalyzes the silanol condensation reaction. Thus, in the presence of amine curing agents, the healing agents will react prematurely and will therefore not be available to flow into and polymerize in the site of damage during a healing event. To overcome this limitation, and provide a more chemically stable and versatile approach, the HOPDMS/PDES healing agent blend was successfully encapsulated using the standard urea-formaldehyde encapsulation procedure already described (22,46). A second limitation is the need for elevated temperatures to be used (50°C) for appreciable self-healing to be observed. To address this concern, a more efficient polycondensation catalyst, tetrakis(acetoxydibutyltinoxy)silane ($Si[OSn(n\text{-}C_4H_9)_2OOCCH_3]_4$, TKAS), was synthesized, encapsulated using the polyurethane encapsulation procedure described above and used in self-healing experiments instead of DMDNT. In addition to its room-temperature activity, unlike DMDNT and DBTL, this catalyst does not require moisture for activation; potentially enabling the design of self-healing coatings for moisture-free environments such as found in aerospace or at buried interfaces. The corrosion-resistance performance of the dual-capsule system was demonstrated in both, a standard epoxy resin applied on a steel substrate as a coating, and in a commercial epoxy marine coating system. For both systems, 3 wt% TKAS catalyst-filled polyurethane capsules, 14 wt% HOPDMS/PDES healing agent blend microcapsules, and 3 wt% adhesion promoter were added to the appropriate matrix. A set of control samples were similarly prepared, but excluding the self-healing additives. Control and

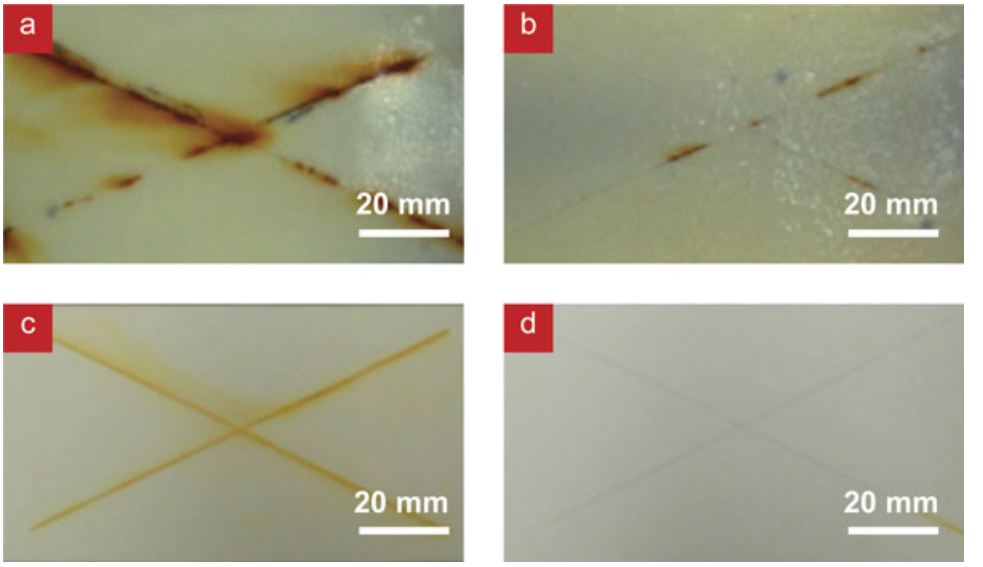

Fig. 14. Commercial marine epoxy coating containing (**a**) adhesion promoter coated on a steel substrate; (**b**) HOPDMS, PDES, and adhesion promoter; (**c**) TKAS catalyst microcapsules and adhesion promoter; (**d**) the complete self-healing system including HOPDMS, PDES, adhesion promoter, and TKAS catalyst microcapsules. All samples were healed at room temperature (approximately 25°C).

self-healing samples were scribed by hand as previously described, allowed to heal for 24 hours at room temperature and then exposed to a 5 wt% sodium chloride solution for 120 hours. The results obtained in this case were consistent with those observed in Figure 13 when the samples were healed at 50°C. All controls exhibited some rusting in and around the scribed region while the sample with the self-healing additive did not display any visible rusting (Fig. 14).

Applications in Reinforced Polymer Composites. The successful demonstration of self-healing in epoxy-based coatings led to studies on the use of this system in the design of more economical self-healing reinforced composites. Preliminary TDCB experiments in neat epoxy resin showed that samples containing the dual-capsule system of HOPDMS/PDES healing agents and microencapsulated organotin catalyst exhibited fracture toughness recovery ranging from 11% to 39% depending on the molecular weight of the PDMS resin used, the concentration of healing agent and catalyst microcapsules, and the use of adhesion promoters (47). A potential application for this healing chemistry is in the design of self-healing composites for cryogenic storage tanks, where healing of microcracks could be induced by failure stemming from use-associated thermal cycling. Moll and co-workers have evaluated the ROMP-based self-healing system for this application with very impressive results (48). However, as was previously discussed the cost of Grubbs' catalysts might preclude the use of this chemistry in practical applications. In preliminary tests, designed to evaluate the feasibility of PDMS polycondensation chemistry for the design of self-healing cryogenic tanks, a self-healing glass fiber-reinforced epoxy composite was fabricated along with the neat

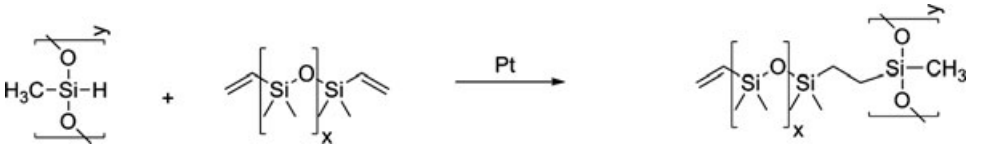

Fig. 15. Hydrosilylation of vinyl-terminated PDMS. A vinyl-terminated PDMS chain reacts with an active methylhydrosiloxane in the presence of a platinum catalyst to yield a crosslinked network.

resin composite control sample. These samples were subsequently damaged by indentation and then tested in a specially-designed pressure cell for air leakage. The self-healing composite exhibited 100% self-sealing capability compared to the neat resin controls in which nearly all samples exhibited significant leakage (49).

Platinum–Catalyzed Hydrosilylation. An alternative PDMS chemistry that has been used in the development of self-healing polymers is the platinum-catalyzed hydrosilylation of vinyl-terminated PDMS with a methylhydrosiloxane copolymer (Fig. 15). This system was the first self-healing system to be evaluated in an elastomeric coating (PDMS) and it was therefore essential to ensure that the damage mechanisms incurred in an elastomer would lead to rupture of embedded microcapsules and the healing event that typically follows. White and co-workers utilized an Eshelby-Mura equivalent inclusion model to numerically determine how an approaching crack interacts with a microcapsule in a linearly elastic matrix (16). Their analysis revealed that the crack was drawn to the more compliant microcapsule. Keller and co-workers investigated the complex interaction of an embedded microcapsule with the nonlinear elastomeric PDMS matrix under tensile loading (48). A series of microscopic images taken of a single microcapsule embedded in a PDMS matrix loaded in uniaxial, and far-field tension showed that the microcapsule deformed in tandem with the matrix until the bulk stretch of the matrix reached a 50% increase over the original axial dimensions. As the deformation increased beyond this point, the capsule shell wall began to fail within the matrix. Concurrently, the capsule was observed to increase in volume in a fashion similar to void growth. Thus, although urea-formaldehyde is a brittle material with low strain-to-failure in the bulk form, the microcapsule exhibits a large strain prior to failure and is consistent with capsule compression data (49,50).

Although the urea-formaldehyde microcapsules are robust in the highly elastic PDMS matrix, an approaching tear does rupture the microcapsules. Keller and co-workers observed ruptured microcapsules in the failure plane of a PDMS sample by scanning electron microscopy (49). Additionally, and somewhat analogous to previous work in epoxy matrices (31), they observed that the addition of microcapsules had a modest reinforcing effect on the tear strength of the PDMS matrix, as the tear energy for a sample containing 20 wt% microcapsules increased about 25% over the neat PDMS material. Perhaps more importantly however, no degradation in the tear strength was observed with the addition of microcapsules.

Evaluation of Self-Healing Performance. Keller and co-workers evaluated; the autonomic healing of tear damage in PDMS samples of four varieties

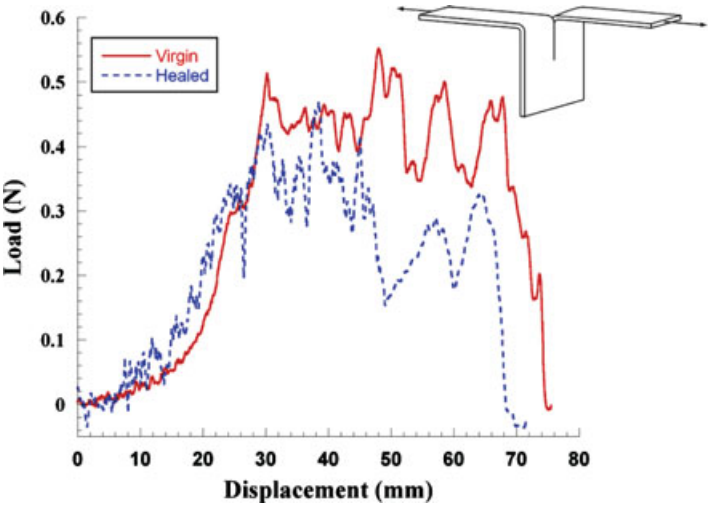

Fig. 16. Representative load-displacement data for a virgin (solid line) and healed (dashed line) tear test of a self-healing PDMS sample with 10 wt% resin microcapsules and 5 wt% curing agent microcapsules. The healing efficiency for this sample was 76% after healing at room temperature (approximately 25°C) for 48 hours. Inset: tear specimen geometry. Reprinted from M.W. Keller, S.R. White, and N.R. Sottos, *Adv. Funct. Mater*. **17**, 2399–2404 (2007) with permission from Wiley-VCH Verlag GmbH & Co. KGaA.

including the neat PDMS matrix with no self-healing additives, reference samples in which PDMS prepolymer was injected after the tear damage, self-activated samples in which one component was included in the matrix and the second was injected, and fully *in situ* samples which were dual-capsule samples containing both initiator and resin microcapsules. All samples were molded into the geometry shown in Figure 16 (inset). The healing efficiency was defined as the recovery of tear strength in the healed sample compared to the initial virgin sample as shown in Equation (4), (49)

$$\eta = \frac{T_{\text{healed}}}{T_{\text{virgin}}} = \frac{F^{\text{avg}}_{\text{healed}}}{F^{\text{avg}}_{\text{virgin}}} \tag{4}$$

where T is the tear strength in the virgin and healed states. The tear strength as defined by the well-known analysis of Rivlin and Thomas for this tear sample is a function of the thickness of the sample (51). The sample thickness remains unchanged between the virgin and the healed tests and the healing efficiency (η) could be reduced to the ratio of the average tearing forces for the healed and virgin tests as shown in Equation (4). Representative load-displacement data for virgin and healed tear tests for a fully *in situ* sample are shown in Figure 16. Average healing efficiencies for the fully *in situ* samples containing 5 wt% initiator capsules and 5–20 wt% resin capsules ranged from 70% to 120%. Healing efficiencies greater than 100% are the result of the deviation of the tear through the healed sample, away from the original tear through the virgin sample, since the original tear path presents a tougher path for the propagating tear relative

to the original virgin material. When a tear deviation occurs, the tear essentially propagates through virgin, previously undamaged material. If the healing of the sample is so complete that the tear in the healed samples deviates away from the original virgin sample tear, then the healing efficiency can be 100% or greater (49).

Application to Self-Healing Coatings. Wilson and co-workers applied the hydrosilylation self-healing chemistry in the design of novel self-healing coatings (52). Microcapsules similar to those prepared by Keller and co-workers were prepared and evaluated in polyurethane clear coat samples and finished silicone coatings. A specified amount of curing agent microcapsules (0–10 wt%) and resin microcapsules (0–20 wt%) were added directly to a specified coating system and mixed thoroughly, prior to applying on previously belt-sanded and solvent-wiped ASTM-specified cold-rolled steel substrates. The samples were then scribed either by hand or by a test panel scratcher and allowed to heal for 24 hours prior to exposure in a salt-fog according to ASTM B117. In general, for both polyurethane and silicone coatings, control samples which did not contain any self-healing additives exhibited significant rusting and blistering in and around the scribe, while samples containing both resin and curing agent microcapsules exhibited self-healing functionality, no blistering and thus continued protection of the substrate. Figure 17 shows a comparison of the control and self-healing samples from the test performed using a polyurethane clear coating system. A comparison of the undercut due to corrosion creepage from the scribed region for a series of samples coated with the polyurethane self-healing coating relative to the control samples, exhibited a significant improvement in corrosion resistance due to the presence of the self-healing additives in the coating. Using the corrosion rating system

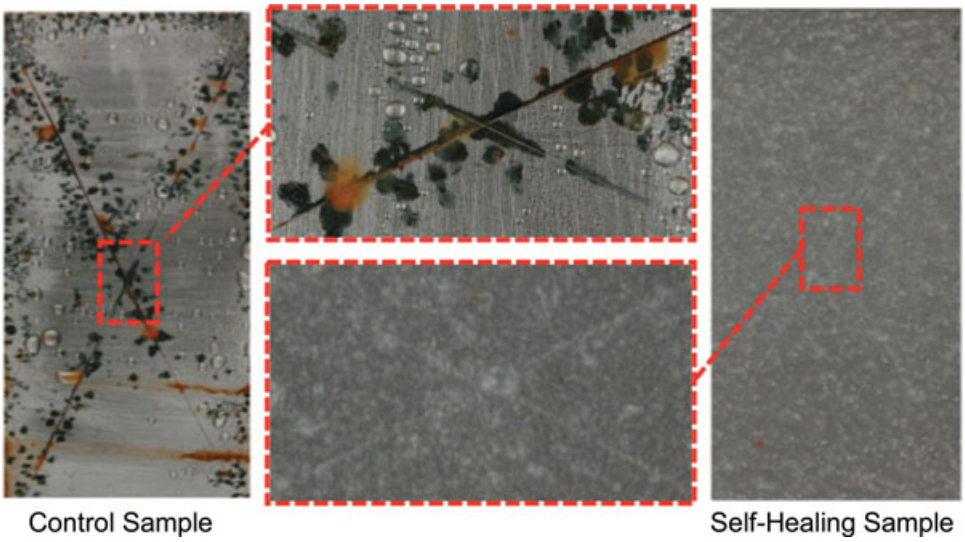

Fig. 17. Results from salt fog corrosion tests after 120 hours exposure according to ASTM B117 of cold-rolled steel samples coated with a polyurethane coating containing no self-healing additives (control sample: left and top center) and with the self-healing additives included (self-healing sample: right and bottom center).

described in ASTM 1654 for evaluating corrosion at the scribed region, the self-healing performance of the coating was defined in terms of the life extension provided as follows:

$$\lambda_{C.R.} = \frac{R_{S.H.} - R_C}{R_C} \times 100\% \tag{5}$$

where $\lambda_{C.R.}$ is the healing efficiency determined from the corrosion ratings, $R_{S.H.}$ is the corrosion rating assigned to the self-healing sample, and R_C is the corrosion rating assigned to the control sample. For coating samples that were approximately 500 μm thick, the healing efficiency was observed to be heavily dependent on microcapsule concentration with healing efficiencies of 200 and 300% observed for samples containing a total of 20 and 40 wt% of microcapsules, respectively. For all these samples, the ratio of curing agent microcapsules to resin microcapsules was 1:9.

Hollow Fiber and Microvascular Network-based Systems. A major limitation to microencapsulation-based self-healing systems is that rupture of a microcapsule depletes the healing agent contained within it. Self-healing using this approach limits the number of times that damage to the same region of the material can be healed. Looking at biological models for inspiration, the vascular system appears to be the solution as it continually replenishes the host material with the chemical building blocks for healing.

Hollow-Fiber Systems. The storage of healing agents in hollow fibers embedded in composite material systems represent a first generation approach for replicating the biological vascular system in a material (53–57). An example of this approach is the work by Pang and Bond, whose work served the dual purpose of highlighting typically barely visible impact damage in composites as well as healing the damage when it occurs (53,54). One set of hollow glass fibers were filled with a blend of a modified epoxy resin repair agent and a UV fluorescent dye, while the other set were filled with the corresponding epoxy resin hardener. These two sets of fibers were incorporated in plies that were assembled at a 90° angle to each other as a part of the complete composite system, which also included solid fibers. The resulting composite material was then cut into specimens of specified geometries for impact and subsequently flexural testing. A comparison of the indentation of self-healing samples which contained the repair agent-infiltrated fibers and control samples which contained no repair agents showed no significantly different load-displacement response; and recovery of flexural strength of up to 97% was confirmed for the self-healing sample in four-point bend flexural tests. Figure 18 shows the various damage mechanisms incurred due to indentation. Additionally, for samples subjected to flexure until failure, the release of dye from within the fractured hollow fiber was visually observed under a UV light source, thus demonstrating the feasibility of the dye release as a method for damage visualization (Fig. 19) (54). This approach has also been successfully demonstrated in carbon fiber-reinforced composites (55,56), and formed the basis for more recent work on self-healing sandwich panels based on vascular networks formed from similar hollow fibers (57).

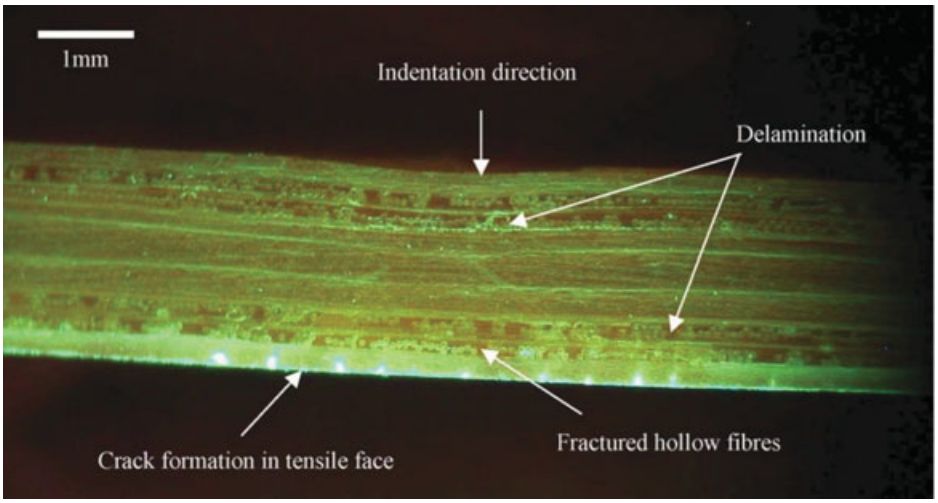

Fig. 18. Optical micrograph of cross-section through impact-damaged hybrid glass/epoxy laminate containing solid and hollow fibers. Some of the hollow fibers were filled with an epoxy resin and a UV-fluorescent dye, while the remaining hollow fibers were filled with the corresponding curing agent. Reprinted from J.W.C. Pang and I.P. Bond, *Composites A*, **36**, 183–188 (2005) with permission from Elsevier.

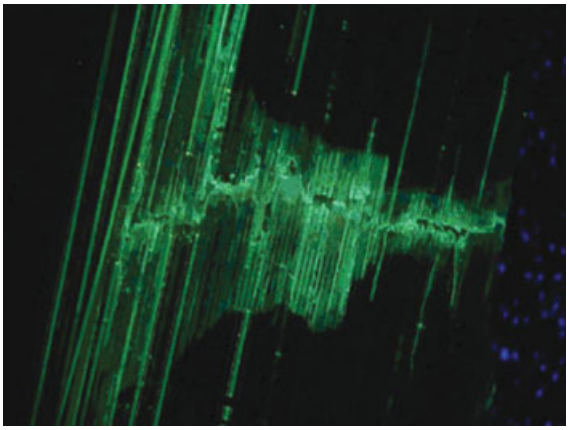

Fig. 19. Fractured region of a hybrid solid/hollow fiber reinforced composite observed under a UV light source showing release of UV fluorescent dye along the crack paths. Reprinted from J.W.C. Pang and I.P. Bond, *Composites A* **36**, 183–188 (2005) with permission from Elsevier.

Microvascular Systems. Truly vascular systems present the challenge of designing and fabricating a pervasive, interconnected, three-dimensional (3D) vascular network across multiple length scales (58–63). While the complexity and level of interconnectivity in natural systems is formidable to replicate in materials systems, simplified networks have been designed, fabricated, and tested. Therriault and co-workers demonstrated an impressive degree of mixing in 3D microvascular networks fabricated by direct-write assembly of a fugitive organic

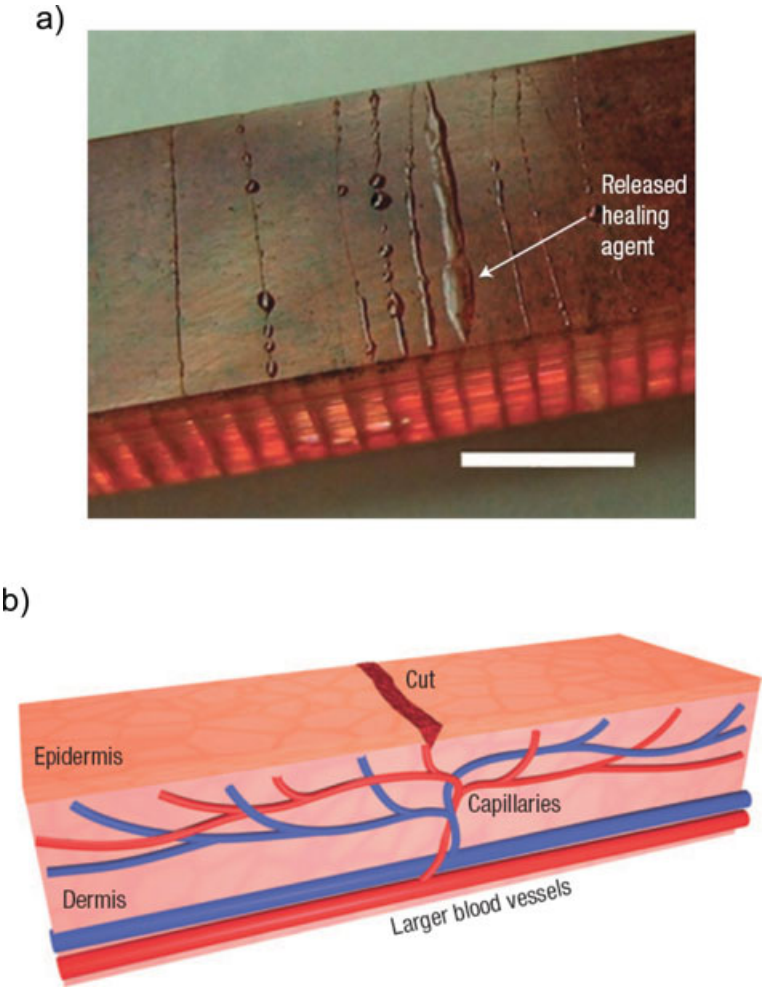

Fig. 20. (**a**) Optical image of a self-healing sample containing a microvascular network substrate after cracks are formed in the epoxy coating, showing the release of the healing agent from the cracks (Scale bar = 5 mm); (**b**) schematic diagram of a capillary network in the dermis layer of skin with a cut in the epidermis layer. Reprinted from K.S. Toohey, N.R. Sottos, J.A. Lewis, J.S. Moore and S.R. White, *Nature Materials*, **6**, 581–585 (2007) with permission from Macmillan Publishers Ltd.

ink (58). Toohey and co-workers utilized similarly fabricated microvascular networks to demonstrate the feasibility of autonomic repair of repeated damage events (59). This demonstration of self-healing via a microvascular approach is shown in Figure 20**a** where it is compared to the capillary network in the dermis layer of the skin (Fig. 20**b**) from which it is inspired. An epoxy coating (about 700 μm thick) was deposited on the more ductile 3D microvascular network. Solid catalyst particles were embedded in the epoxy coating and the network was filled with DCPD. The resulting coating-substrate beam was then loaded in four-point bending until crack initiation occurred at the surface of the coating where the

tensile stress is greatest. After damage has occurred in the coating, the healing agent flows from the channels in the vascular network into the cracks by capillary action. As with microcapsule-based systems, once in the crack plane, the healing agent reacts with the embedded catalyst particles in the coating to initiate polymerization and rebond the crack faces autonomically.

Evaluation of Self-healing Performance. For mechanical testing and evaluation of self-healing performance, the coating-substrate beams were loaded in four-point bending to initiate a single crack in the coating without damaging the underlying microvascular substrate. An acoustic emission sensor was placed on the beam being tested to detect the crack opening events during the experiment. The time at which the critical acoustic-emission event occurred was used to determine the peak fracture loads of crack formation and reopening in the virgin and healed specimens. The healing efficiency is calculated for each healing cycle on the basis of the ratio of the critical loads for crack opening. As was the case for the microencapsulation-based self-healing systems described above, the healing efficiency is defined as the ratio of the peak fracture load of the healed sample to that of the virgin sample. In the evaluation of the four-point test, the fracture toughness for the first crack is the virgin fracture toughness ($K_{ICvirgin}$) to which the fracture toughness of the healed sample ($K_{IChealed}$) is compared. Also as with fracture testing of TDCB samples, the material properties and geometry of a single specimen do not change and the healing efficiency can therefore be reduced to the ratio of the peak fracture loads as was illustrated in Equation (1). Samples containing the highest catalyst concentration tested (10 wt%) exhibited healing over the largest number of loading cycles. Healing efficiencies from these tests reported by Toohey and co-workers ranged from just less than 60% after the first loading cycle to approximately 45% after the seventh and final loading cycle. The highest healing efficiency recorded was 70% and it was recorded after the second loading cycle and the lowest healing efficiency recorded was just less than 35% recorded after the fourth loading cycle (59). Toohey and co-workers also developed microvascular-based self-healing systems using two-part epoxy chemistry (61). Healing efficiencies of over 60% were achieved for up to 16 intermittent healing cycles of a single crack.

Self-Healing Ionomers. Based on the definition of self-healing polymers given in the Introduction Section, the healing of ionomers after ballistic impact can be defined as autonomic self-healing to the extent that no additional energy is supplied to facilitate self-healing. Ionomers are a class of polymers that contain ionic species incorporated into the structure of the organic polymer, thus creating interactions that are not present in comparable nonionic polymers. These interactions yield mechanical and physical properties that have been the subject of much research in academia and industry (64). Until recently however, comparatively little research has been carried out to elucidate the self-healing functionality of ionomers.

Self-healing in ionomeric systems is activated during high energy impact. This is a very unique case in which the type of damage and damage conditions must work synergistically with the polymeric structure for optimal self-healing properties to be observed. The self-healing process has been summarized as follows (64):

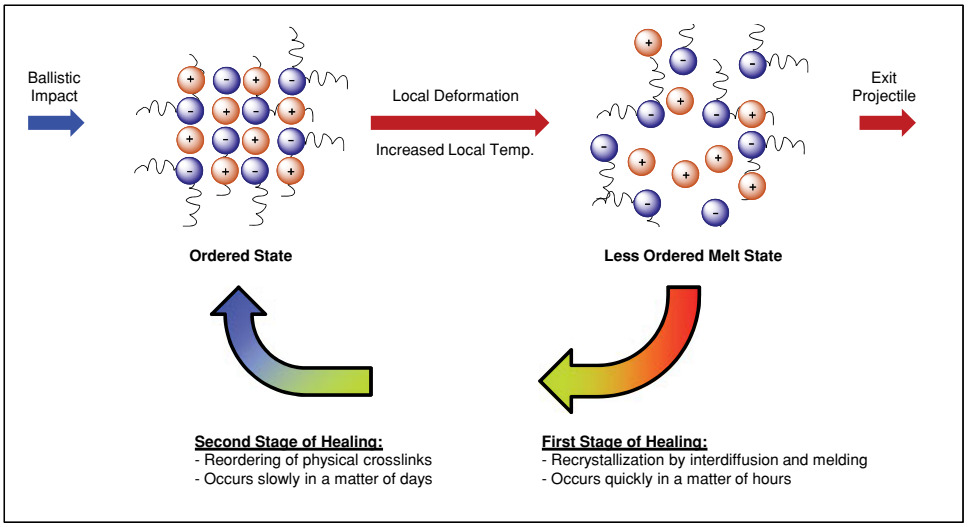

Fig. 21. Schematic summarizing the healing of ballistic impact damage in an ionomer.

(1) Impact—The high speed impact of a projectile transfers energy to the polymer both elastically (energy is stored) and inelastically (energy dissipates). Localized temperature increases due to frictional effects from the impact, causing the polymeric material in the local vicinity to move from an ordered state to a disordered melt state.

(2) Deformation—The elasticity of the melt state allows the polymer to be drawn to significant strain levels before failure and exit of the projectile. The uncompromised regions of the polymer elastically rebound to its original position prior to impact.

(3) Healing—The fragments of the polymer in the melt state are able to interdiffuse together to heal the cavity and over a longer period of time, the strength of the compromised region of the polymer returns as the crosslinks reorder.

The self-healing steps described above are illustrated in Figure 21. An attempt at quantifying the healing efficiency of similar ionomeric materials was made using tensile dog bone specimen that had been cut into two pieces and heated locally above the melting point of the ionomer. After a period of time, the two pieces of the samples were brought back together, cooled rapidly, loaded at a constant rate of displacement and heated at a specified temperature for a specified length of time. Healing efficiencies ranging from 56% ($T = 138^{\circ}$C, $t = 0$) up to 90% ($T = 138^{\circ}$C, $t = 500$ seconds) were observed (64). It is important to note however, that these results were obtained from experiments that isolated the viscous or nonelastic contribution to the overall self-healing mechanism of ionomers. This type of healing of a materials system by introducing energy from an external source is classified as nonautonomic healing.

Nonautonomic Systems

The rapid growth of the field of self-healing polymeric materials has also led to some interesting and insightful chemistries that while not entirely autonomic do add to the portfolio of chemistries that can be used in the design of smarter responsive materials. Wudl and co-workers have performed extensive research on the use of Diels–Alder and retro-Diels–Alder reactions in the design of remendable polymeric materials (65,66). Multifunctional furan and maleimide-based monomers were used to form highly cross-linked polymer networks via Diels-Alder step-growth polymerization. When subject to repeated healing and cooling cycles, solid state ^{13}C NMR spectroscopy studies confirmed the occurrence of the retro-Diels-Alder reaction at 120°C. Samples of these polymers were stressed to failure and subsequently repaired by heating in the 90–120°C range followed by cooling to room temperature. A recovery of almost 60% of the original material strength was recorded in the initial demonstration of this approach (65), with an improved version of the same system recording greater than 80% recovery under similar conditions (66).

Continuing with the theme of thermally-induced healing in materials, Balijepalli and co-workers have reported preliminary results on polyurethane resin systems with the ability to self-repair under mild thermal conditions (67). These polyurethane resin systems incorporated hydrophobic natural oil polyols with controlled equivalent weight as a mean of controlling the crosslink density of the resulting polyurethane network. The glass transition temperatures (T_g) of the polymers made were in the range of 40–50°C. When coated on glass and heated to 10°C above their respective T_g's (50–60°C) these polyurethane samples exhibited recovery of scratch depth ranging from 20% to almost 100% in a time frame ranging from 20–120 minutes. A similar approach was taken by Bayer Materials Science AG and is also being adopted by various automotive paint suppliers (68).

A recently reported example of nonautonomic healing is the work by Ghosh and Urban on self-repairing oxetane-substituted chitosan polyurethane networks, which exhibit self-repairing characteristics upon exposure to UV light (69). Upon mechanical damage, the strained four-member oxetane rings open presumably by homolytic cleavage to create two reactive ends. When exposed to UV light in the appropriate wavelength, chitosan chain scission occurs resulting in a crosslinking reaction with the reactive oxetane ends thus repairing the network. Scratches of approximately 10 μm were completely repaired upon exposure to UV light (280–400 nm) for 30 minutes.

BIBLIOGRAPHY

1. R. P. Sheldon, *Composite Polymeric Materials*; Applied Science Publishers: Essex, UK, 1982.
2. E. K. Gamstedt and R. Talreja, *Journal of Materials Science* **34**, 2535–2546 (1999).
3. R. P. Wool and K. M. O'Connor, *J. Appl. Phys.* **52**, 5953–5963 (1981).
4. K. Jud and H. H. Kausch, *Polymer Bulletin* **1**, 697–707 (1979).
5. C. B. Lin, S. Lee, and K. S. Liu, *Polym. Eng. Sci.* **30**, 1399–1406 (1990).
6. Y. H. Kim and R. P. Wool, *Macromolecules* **16**, 1115–1120 (1983).

7. S. Prager and M. Tirrell, *J. Chem. Phys.* **75**, 5194–5198 (1981).
8. R. P. Wool, *ACS Polym. Prepr.* **23**, 62–65 (1982).
9. S. S. Voyutskii, *Autoadhesion and Adhesion of High Polymers*, Wiley, New York, 1963.
10. C. B. Lin, S. Lee, and K. S. Liu, *Polym. Eng. Sci.* **30**, 1399–1406 (1990).
11. P. Wang, S. Lee, and J. P. Harmon, *J. Polym. Sci. B* **32**, 1217–1227 (1994).
12. H. Hsieh, T. Yang, and S. Lee, *Polymer* **42**, 1227–1241 (2001).
13. C. B. Lin, S. Lee, and K. S. Liu, *J. Adhesion* **34**, 221–240 (1991).
14. C. B. Lin, S. Lee, and K. S. Liu, *J. Polym. Sci B* **29**, 1457–1466 (1991).
15. C. Dry, *Compos. Struct.* **35**, 263–269 (1996).
16. S. R. White, N. R. Sottos, P. H. Geubelle, J. S. Moore, M. R. Kessler, S. R. Sriram, E. N. Brown, and S. Viswanathan, *Nature* **409**, 794–797 (2001).
17. S. Sriram, Ph.D. Thesis, University of Illinois at Urbana-Champaign, 2001.
18. J. D. Rule, Ph.D. Thesis, University of Illinois at Urbana-Champaign, 2005.
19. R. H. Grubbs, W. Tumas, *Science* **243**, 907–915 (1989).
20. P. Schwab, R. H. Grubbs, and J. W. Ziller, *J. Am. Chem. Soc.* **118**, 100–110 (1996).
21. M. S. Sanford, L. M. Henling, and R. H. Grubbs, *Organometallics* **17**, 5384–5389 (1998).
22. E. N. Brown, M. R. Kessler, N. R. Sottos, and S. R. White, *J. Microencapsulation* **20**, 719–730 (2003).
23. E. N. Brown, N. R. Sottos, and S. R. White, *Exp. Mech.* **42**, 372–379 (2002).
24. B. J. Blaiszik, N. R. Sottos, and S. R. White, *Compos. Sci. Tech.* **68**, 978–986 (2008).
25. G. O. Wilson, M. M. Caruso, N. T. Reimer, S. R. White, N. R. Sottos, and J. S. Moore, *Chem. Mater.* **20**, 3288–3297 (2008).
26. G. O. Wilson, K. A. Porter, H. Weissman, S. R. White, N. R. Sottos, and J. S. Moore, *Adv. Synth. Catal.* **351**, 1817–1825 (2009).
27. A. S. Jones, J. D. Rule, J. S. Moore, S. R. White, and N. R. Sottos, *Chem. Mater.* **18**, 1312–1317 (2006).
28. E. N. Brown, S. R. White, and N. R. Sottos, *Compos. Sci. Tech.* **65**, 2466–2473 (2005).
29. E. N. Brown, S. R. White, and N. R. Sottos, *Compos. Sci. Tech.* **65**, 2474–2480 (2005).
30. A. S. Jones, J. D. Rule, J. S. Moore, N. R. Sottos, and S. R. White, *J. R. Soc. Interface* **4**, 395–403 (2007).
31. E. N. Brown, S. R. White, and N. R. Sottos, *J. Mater Sci.* **39**, 1703–1710 (2004).
32. M. R. Kessler and S. R. White, *Composites: Part A* **32**, 683–699 (2001).
33. M. R. Kessler and S. R. White, *Composites: Part A* **34**, 743–753 (2003).
34. A. J. Patel, N. R. Sottos, E. D. Wetzel, and S. R. White, *Composites A*, **41**, 360–368 (2010).
35. J. D. Rule, E. N. Brown, N. R. Sottos, S. R. White, and J. S. Moore, *Adv. Mater.* **17**, 205–208 (2005).
36. J. D. Rule and J. S. Moore, *Macromolecules* **35**, 7878–7882.
37. T. C. Mauldin, J. D. Rule, N. R. Sottos, S. R. White, and J. S. Moore, *J. R. Soc. Interface* **4**, 389–393 (2007).
38. E. N. Brown, Ph.D Thesis, University of Illinois at Urbana-Champaign, 2003.
39. G. O. Wilson, J. S. Moore, S. R. White, N. R. Sottos, and H. M. Andersson, *Adv. Funct. Mater.* **18**, 44–52 (2008).
40. G. O. Wilson, K. A. Porter, H. Weissman, S. R. White, N. R. Sottos, and J. S. Moore, *Adv. Synth. Catal.* **351**, 1817–1825 (2009).
41. J. M. Kamphaus, J. D. Rule, J. S. Moore, N. R. Sottos, and S. R. White, *J. R. Soc. Interface* **5**, 95–103 (2008).
42. J. D. Rule, N. R. Sottos, and S. R. White, *Polymer* **48**, 3520–3529 (2007).
43. M. M. Caruso, D. A. Delafuente, V. Ho, N. R. Sottos, J. S. Moore, and S. R. White, *Macromolecules* **40**, 8830–8832 (2007).

44. M. M. Caruso, B. J. Blaiszik, S. R. White, N. R. Sottos, and J. S. Moore, *Adv. Funct. Mater.* **18**, 1898–1904 (2008).
45. S. Cho, H. M. Andersson, S. R. White, N. R. Sottos, and P. V. Braun, *Adv. Mater.* **18**, 997–1000. (2006).
46. S. Cho, S. R. White, and P. V. Braun, *Adv. Mater.* **21**, 645–649 (2009).
47. C. L. Mangun, A. C. Mader, J. L. Moll, N. R. Sottos, and S. R. White, *Proceedings of the 2nd International Conference on Self-Healing Materials*, Chicago, IL, U.S.A., June 2009.
48. J. L. Moll, S. R. White, and N. R. Sottos, *J. Compos. Mater.* 2010, Online.
49. M. W. Keller, S. R. White, and N. R. Sottos, *Adv. Funct. Mater.* **17**, 2399–2404 (2007).
50. M. W. Keller and N. R. Sottos, *Exp. Mech.* **46**, 725–733 (2006).
51. R. S. Rivlin and A. G. Thomas, *J. Polym. Sci.* **10**, 291–295 (1953).
52. G. O. Wilson and H. M. Andersson, *Proceedings of the 2nd International Conference on Self-Healing Materials*, Chicago, IL, U.S.A., June 2009.
53. J. W. C. Pang and I. P. Bond, *Composites A* **36**, 183–188 (2005).
54. J. W. C. Pang and I. P Bond, *Compos. Sci. Tech.* **65**, 1791–1799 (2005).
55. G. J. Williams, R. S. Trask, and I. P. Bond, *Composites A* **38**, 1525–1532 (2007).
56. H. R. Williams, R. S. Trask, and I. P. Bond, *Compos. Sci. Tech.* **68**, 3171–3177 (2008).
57. G. J. Williams, I. P. Bond, and R. S. Trask, *Composites A* **40**, 1399–1406 (2009).
58. D. Therriault, S. R. White, and J. A. Lewis, *Nature Materials* **2**, 265–271 (2003).
59. K. S. Toohey, N. R. Sottos, J. A. Lewis, J. S. Moore, and S. R. White, *Nature Material* **6**, 581–585 (2007).
60. K. S. Toohey, N. R. Sottos, and S. R. White, *Exp. Mech.* **49**, 707–717 (2009).
61. K. S. Toohey, C. J. Hansen, J. A. Lewis, S. R. White, and N. R. Sottos, *Adv. Funct. Mater.* **19**, 1399–1405 (2009).
62. C. J. Hansen, W. Wu, K. S. Toohey, N. R. Sottos, S. R. White, and J. A. Lewis, *Adv. Funct. Mater.* **21**, 1–5 (2009).
63. A. R. Hamilton, N. R. Sottos, and S. R. White, *Exp. Mech.* published online (2009) DOI: 10.1007/S11340-009-9299-5.
64. R. Varley, In Self-Healing Materials, S. van der Zwaag, ed., *Springer Series in Materials Science 100*, Springer, Dordrecht, The Netherlands, 2007; pp 95–113.
65. X. Chen, M. A. Dam, K. Ono, A. K. Mal, H. Shen, S. R. Nutt, K. Sheran, and F. Wudl, *Science* **295**, 1698–1702 (2002).
66. X. Chen, F. Wudl, A. K. Mal, H. Shen, and S. R. Nutt, *Macromolecules* **36**, 1802–1807 (2003).
67. S. Balijepalli, K. Nanjundiah, Y. Li, and M. Barsacchi, Proceedings of the European Coatings Conference, Nuremberg, Germany, April 2009.
68. R. A. van Benthem, W. Ming, and G. de With, In Self-Healing Materials, S. van der Zwaag, ed., *Springer Series in Materials Science 100*, Springer, Dordrecht, The Netherlands, 2007; pp 139–159.
69. B. Ghosh and M. W. Urban, *Science* **323**, 1458–1460 (2009).
70. R. H. Grubbs, ed., *Handbook of Metathesis*, Vol. **1–3**, Wiley–VCH, Weinheim, Germany, 2003.
71. S. Van Der Zwaag, ed., *Self-Healing Materials*, Springer, Dordrecht, The Netherlands, 2007.
72. S. K. Ghosh, ed., *Self-Healing Materials*, Wiley-VCH Verlag GmbH & Co. KGaA, Weinheim, Germany, 2009.
73. S. K. Ghosh, ed., *Functional Coatings*, Wiley-VCH Verlag GmbH & Co. KGaA, Weinheim, Germany, 2006.

GERALD O. WILSON
H. MAGNUS ANDERSSON
Autonomic Materials, Inc
Champaign, Illinois

SCOTT R. WHITE
NANCY R. SOTTOS
JEFFREY S. MOORE
PAUL V. BRAUN
University of Illinois at Urbana-Champaign
Urbana, Illinois